

MONAZITE AGES BY THE CHEMICAL Th-U-TOTAL Pb ISOCHRON METHOD FOR PELITIC GNEISSES FROM THE EASTERN SØR RONDANE MOUNTAINS, EAST ANTARCTICA

Masao ASAMI¹, Kazuhiro SUZUKI² and Mamoru ADACHI²

¹*Department of Earth Sciences, Faculty of Science, Okayama University,
1-1, Tsushima-naka 3-chome, Okayama 700*

²*Department of Earth and Planetary Sciences, School of Science, Nagoya University,
Furocho, Chikusa-ku, Nagoya 464-01*

Abstract: Chemical Th-U-total Pb isochron (CHIME) ages were determined with an electron microprobe analyzer on 14 to 24 monazite grains in three garnet-biotite gneisses collected from separate outcrops in the eastern part of the Sør Rondane Mountains, East Antarctica. On the basis of geologic and petrologic studies, investigators have inferred a two-stage metamorphic history for the Sør Rondane: (1) an earlier regional granulite-facies event inferred from U-Pb zircon and Rb-Sr and Sm-Nd whole rock data to be ~1000 Ma in age, and (2) an amphibolite-facies overprint inferred to be ~500 Ma in age. PbO-ThO₂* plots based on ThO₂, UO₂ and PbO contents of monazites yield a well-defined isochron for each gneiss, although both matrix grains in all gneiss samples and inclusions in garnet and pyrrhotite grains in a sample were analyzed. The isochrons give 536, 534 and 534 Ma ages, indicating a single crystallization age (~535 Ma) for the monazites. This age is in good agreement with the ~500 Ma age currently assigned to the amphibolite-facies overprint. However, the high Pb retentivity reported for monazite, along with textural and mineralogical characteristics of the samples, constrains assignment of the monazite age to the granulite-facies metamorphism rather than to retrograde recrystallization. Our ~535 Ma ages give rise to a possibility of further westward extension of a Cambrian orogenic belt recently reported from the Lützow-Holm and Yamato-Belgica Complexes, where a similar succession of metamorphic and plutonic activities has been recognized.

key words: CHIME age, monazite, Cambrian, granulite facies, Sør Rondane Mountains

1. Introduction

The Sør Rondane Mountains (71.5–72.5°S, 22–28°E) in the East Antarctic shield are underlain by a high-grade regional metamorphic complex that is intruded by various kinds of plutonic rocks and minor dikes (VAN AUTENBOER and LOY, 1972; SHIRAI SHI *et al.*, 1991; ASAMI *et al.*, 1992). The majority of the metamorphic rocks is of granulite-facies, and shows evidence of subsequent amphibolite-facies recrystallization possibly related to migmatization and plutonism. Most of the geochronologic data so far reported on the metamorphic and plutonic rocks give early Paleozoic ages (*ca.* 500 Ma, *e.g.* PICCIOTTO *et al.*, 1964), but some Rb-Sr and Sm-Nd whole-rock isochron data and U-Pb zircon data give late Proterozoic ages (*ca.* 1000 Ma,

TAKAHASHI *et al.*, 1990; GREW *et al.*, 1992; SHIRAISHI and KAGAMI, 1992). Some may consider the late Proterozoic ages as the time of the regional granulite-facies metamorphism and the Paleozoic ones as the time of the amphibolite-facies event (*e.g.* GREW *et al.*, 1992). However, there is still some room for different interpretation on the late Proterozoic ages; the *ca.* 1000 Ma Rb-Sr and Sm-Nd isochron ages may indicate the time of the protolith formation of the metamorphic rocks. If this is the case, timing of the granulite-facies metamorphism is a particular focus of geologic and geochronologic interest.

Monazite occurs in granulite-facies pelitic gneisses from the Sør Rondane Mountains, and can be used to provide reliable chronologic information about the granulite-facies metamorphic event, because it does not lose significant portions of its Pb even under upper amphibolite-facies conditions (PARRISH, 1990; SMITH and BARREIRO, 1990; SUZUKI *et al.*, 1994). We determined CHIME (chemical Th-U-total Pb isochron method) ages of monazite grains in three pelitic gneisses that were collected by M. ASAMI from the Sør Rondane Mountains during JARE-29, and present the results here. This is the first report on monazite ages from the Sør Rondane.

2. Geologic Setting

The map area occupies the eastern part of the Sør Rondane Mountains (Fig. 1). The geology of this area and petrology of the metamorphic rocks have been reported by GREW *et al.* (1988, 1989a,b, 1991), ASAMI and MAKIMOTO (1991), ASAMI *et al.* (1989, 1990, 1991, 1993, 1994), MAKIMOTO *et al.* (1990) and ISHIZUKA *et al.* (1993), and are briefly summarized below.

The crystalline basement exposed in the area is composed of high-grade gneissic rocks accompanied by migmatite and small bodies of intrusive rocks (Fig. 1). Precursors of the gneissic rocks are sedimentary, volcanogenic and igneous in origin. The majority of the metamorphics are biotite-hornblende gneisses, with subordinate charnockitic gneisses, mafic granulites, amphibolites, cummingtonite-orthopyroxene orthogneiss, pelitic gneisses, marbles, calcsilicate gneisses, quartzite and ultramafic rocks. Regional metamorphism in the granulite facies (760–800°C and 7–8 kb) is indicated by the widespread occurrence of orthopyroxene- and two-pyroxene-bearing assemblages (Fig. 1). The amphibolite-facies overprint at 500–600°C, during which garnet was replaced by biotite and pyroxenes by amphiboles, is recognized as a later event associated with regional migmatization.

3. Analyzed Samples

Three rock samples, containing relatively abundant monazite, were selected for analysis. They are pelitic gneisses collected at three different localities in the map area (Fig. 1):

- (1) garnet-biotite gneiss (MA8801113-3) from the Hesteskøen nunatak,
- (2) gahnite-garnet-biotite gneiss (MA88012305-1) from southern Balchenfjella,
- (3) sillimanite-garnet-biotite gneiss (MA88012912) from the Austhjelmen nunatak.

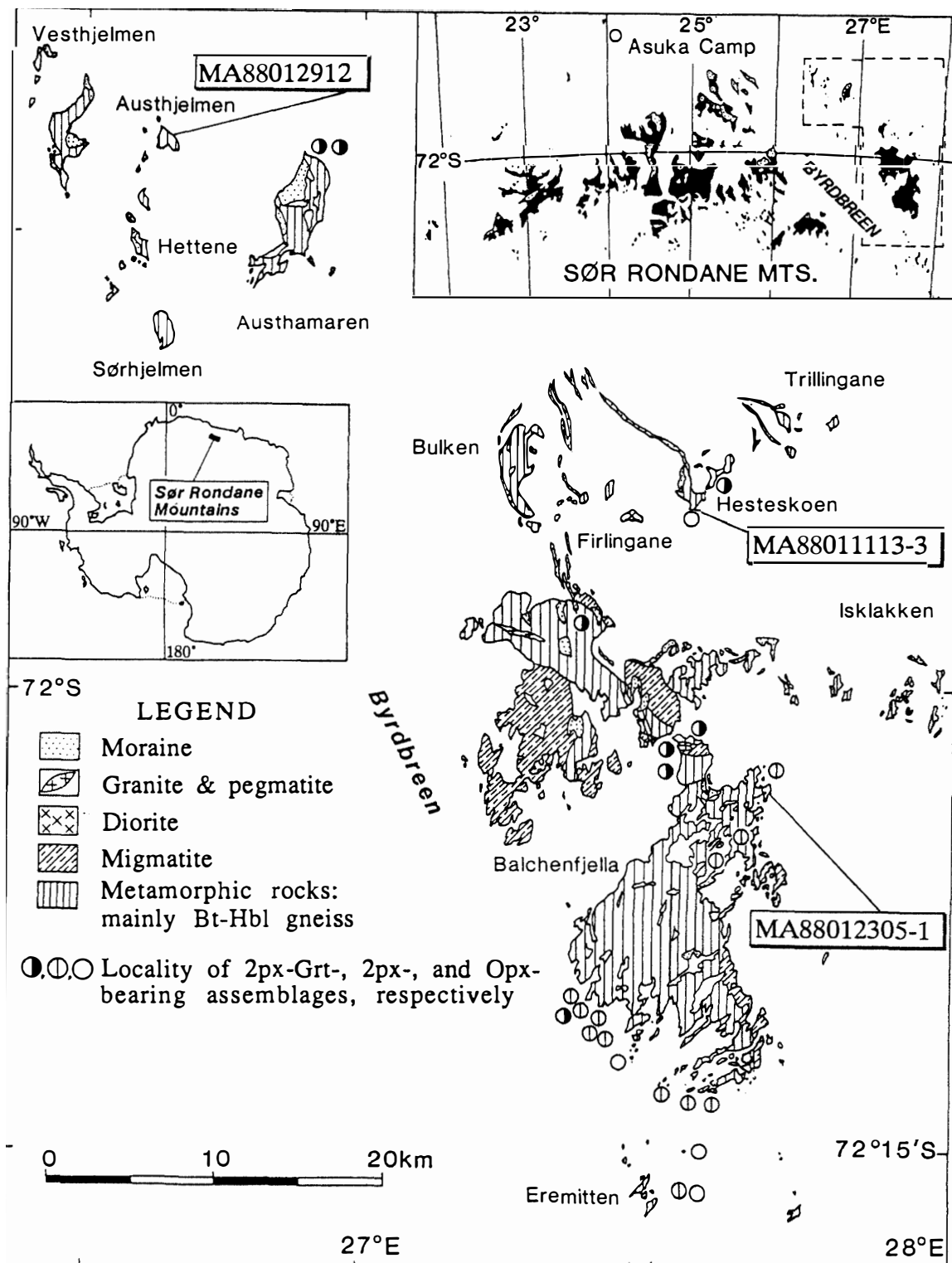


Fig. 1. Simplified geologic map of the eastern Sør Rondane Mountains. Localities of the studied samples (MA8801113-3, MA88012305-1 and MA88012912) are shown together with those of orthopyroxene-bearing assemblages in intermediate and mafic metamorphic rocks. Modified from ASAMI et al. (1989, 1991).

Rocks exposed at Hesteskoen appear to be continuous in lithology and structure with those at Balchenfjella, the largest exposure of the area, and are composed mainly of biotite-hornblende gneiss in which garnet-biotite gneiss and amphibolite are intercalated as layers and lenses. Sample MA88011113-3 is from one of these garnet-biotite gneiss layers. Sample MA88012305-1 is also part of a garnet-biotite gneiss layer intercalated in biotite-hornblende gneiss occurring at the eastern edge of southern Balchenfjella. In the same and nearby exposures of both localities, orthopyroxene-bearing rocks, such as orthopyroxene-garnet-biotite gneiss, two-pyroxene-garnet amphibolite and two-pyroxene-hornblende gneiss, are found (Fig. 1). The field occurrences indicate that the two samples were subjected to the granulite-facies metamorphism.

The Austhjelmen sample, MA88012912, is from a layer of garnet-biotite gneiss alternating with layers of biotite-hornblende gneiss on a fine scale. At Austhjelmen, the sillimanite + K-feldspar association is recognized in some garnet-biotite gneisses, but no orthopyroxene-bearing rock was found. Instead, two-pyroxene-garnet-bearing amphibolite and mafic granulite occur in a nunatak 7 km to the east, Austhamaren, the geologic structure of which is concordant with that of Austhjelmen.

(1) Sample MA88011113-3

This sample is a light brownish gray, indistinctly banded gneiss. It consists of garnet, biotite, K-feldspar, plagioclase, quartz, and accessory apatite, monazite, zircon, iron ore and spinel. Spinel is found in trace amounts enclosed in garnet. Garnet forms small porphyroblasts, less than 1.5 mm in diameter, in a fine- to medium-grained matrix composed of the other minerals. Garnet is locally embayed by biotite-plagioclase aggregates. Garnet and the matrix minerals appear to be in textural equilibrium, whereas the spinel is an armored relic and the aggregates are secondary.

(2) Sample MA88012305-1

This is a dark brownish gray gneiss, but lacking in distinct feldspathic banding. The sample contains gahnite, garnet, biotite, plagioclase and quartz with accessory monazite, apatite, zircon, sphalerite and pyrrhotite. Garnet porphyroblasts, up to 2 mm across, are scattered in a medium-grained matrix of the other constituents. Gahnite ($Zn/(Fe+Mg+Zn)=0.70-0.75$) appears not only as grains in the matrix, but also as small porphyroblasts. Garnet is locally embayed by biotite-plagioclase aggregates. The minerals other than the aggregates are in textural equilibrium.

A compositional profile of an unembayed garnet porphyroblast in this sample was examined using microprobe analyses. The profile shows an almost homogeneous, relatively Mg-rich interior of $X_{Fe}(=Fe/(Fe+Mg))=0.73-0.75$ and a narrow rim with an outward Fe-increase up to $X_{Fe}=0.87$. This type of zoning is characteristic of garnet in pelitic gneisses from this area (ASAMI *et al.*, 1990). The interior is considered to have preserved compositions homogenized during the earlier, granulite-facies event, whereas the Fe-enrichment is considered to have resulted from retrograde Fe-Mg exchange with biotite during the later, amphibolite-facies event. The embayment of garnet is also related to the later event.

(3) Sample MA88012912

The sample is a gray, medium-grained, well-banded gneiss. Constituent minerals

are garnet, biotite, plagioclase, quartz, and accessory sillimanite, monazite, apatite, zircon and iron ore. Garnet is not porphyroblastic but forms euhedral to subhedral grains with no embayment. The minerals are all in textural equilibrium.

In all samples, monazite forms anhedral to subhedral grains up to 0.3 mm in diameter in the matrix. In addition, monazite occurs as inclusions in garnet in the Hesteskoen sample and in garnet and pyrrhotite in the Balchenfjella sample, but no morphological or optical difference can be observed between the matrix grains and inclusions. Thus the formation of monazite is not later than the enclosing minerals. Taking into account the garnet petrogenesis in the Balchenfjella sample, the textural features suggest that monazite in all samples originally crystallized during the granulite-facies metamorphism in association with the other constituents, except for spinel in the Hesteskoen sample and the aggregates in the Hesteskoen and Balchenfjella samples.

4. Experiments

Monazites in polished thin sections were analyzed with a JEOL JXA-733 electron microprobe equipped with three wavelength-dispersive type spectrometers. Operating conditions were 15 kV accelerating voltage, 0.22 μA beam current and 5 μm beam diameter. The ThM_α , UM_β and PbM_β lines were measured at several spots on each grain; no other elements were analyzed. Marginal portions of monazite grains in contact with K-rich phases were not analyzed to avoid the potential spectral interference of KK_α on UM_β . Euxenite provided by SMELLIE *et al.* (1978) was used as a standard for Th and U, and a synthesized glass (56.19% PbO , 13.98% ZnO and 29.21% SiO_2 , analyst: K. HAYASHI) as a standard for Pb. X-ray intensities were integrated over a 300-second period. The measurement was repeated twice or three times, and the arithmetic average of readings was taken. The background was measured at two optimum positions on both sides of each line peak position. Raw intensity data were converted into concentrations by the method described by BENCE and ALBEE (1968) using a composition of Th-rich natural monazite as a reference (10.29% ThO_2 , 0.08% UO_2 and 0.523% PbO ; 0.90% SiO_2 , 0.95% Y_2O_3 , 11.18% La_2O_3 , 27.42% Ce_2O_3 , 2.68% Pr_2O_3 , 12.02% Nd_2O_3 , 2.12% Sm_2O_3 , 0.70% Gd_2O_3 , 0.16% Tb_2O_3 , 0.21% Dy_2O_3 , 1.29% CaO and 28.64% P_2O_5). The slight difference in the matrix elements barely affects the Th, U and Pb determinations; the maximum error in this calculation is around 0.5% of the determinations. This value is less than the uncertainty in the X-ray counting.

5. Results

Analytical results of ThO_2 , UO_2 and PbO together with the apparent age and ThO_2^* value (sum of the measured ThO_2 and ThO_2 equivalent of the measured UO_2) are listed in Tables 1 to 3; the detection limit of PbO at 2σ confidence level is 0.01 wt%, and the relative error in the PbO determination is about 5–10% for 0.1 wt% of the concentration. The CHIME ages were calculated through the method described by SUZUKI and ADACHI (1991a,b, 1994), SUZUKI *et al.* (1991, 1992, 1994) and ADACHI

Table 1. *Microprobe analyses of ThO₂, UO₂ and PbO of monazites in garnet-biotite gneiss (sample: MA8801113-3) from Hesteskoen. ThO₂*: sum of the measured ThO₂ and ThO₂ equivalent of the measured UO₂.*

Grain No.	ThO ₂ (wt%)	UO ₂ (wt%)	PbO (wt%)	Age (Ma)	ThO ₂ * (wt%)	Gain No.	ThO ₂ (wt%)	UO ₂ (wt%)	PbO (wt%)	Age (Ma)	ThO ₂ * (wt%)
M01-01	2.20	0.228	0.069	545	2.96	M08-03	8.59	0.177	0.212	543	9.18
M01-02	2.07	0.232	0.062	514	2.84	M08-04	8.61	0.203	0.212	536	9.28
M01-03	2.54	0.239	0.079	555	3.33	M08-05	8.61	0.211	0.211	532	9.31
M01-04	2.74	0.239	0.078	521	3.53	M08-06	9.13	0.217	0.232	553	9.85
M02-01	2.13	0.184	0.062	533	2.74	M08-07	9.11	0.215	0.221	528	9.82
M02-02	2.01	0.176	0.061	551	2.59	M08-08	9.08	0.220	0.228	546	9.81
M03-01	2.44	0.245	0.073	525	3.25	M09-01	10.3	0.193	0.252	543	10.9
M03-02	2.26	0.243	0.073	555	3.06	M09-02	9.49	0.176	0.227	529	10.1
M03-03	2.43	0.262	0.075	531	3.30	M09-03	10.1	0.190	0.245	534	10.7
M04-01	10.3	0.180	0.247	534	10.9	M09-04	10.5	0.197	0.259	543	11.2
M04-02	10.5	0.196	0.249	524	11.1	M09-05	10.4	0.185	0.252	535	11.0
M04-03	9.91	0.177	0.234	524	10.5	M09-06	9.78	0.199	0.233	523	10.4
M04-04	9.42	0.171	0.226	531	9.99	M09-07	10.6	0.203	0.258	538	11.3
M04-05	10.1	0.181	0.244	536	10.7	M09-08	10.6	0.195	0.258	536	11.2
M04-06	10.3	0.175	0.248	536	10.9	M09-09	9.25	0.187	0.224	532	9.87
M04-07	8.95	0.158	0.212	527	9.47	M09-10	9.79	0.187	0.239	539	10.4
M04-08	9.09	0.198	0.223	537	9.75	M09-11	10.0	0.182	0.244	540	10.6
M04-09	9.93	0.171	0.241	539	10.5	M10-01	9.28	0.213	0.228	537	9.98
M04-10	9.46	0.176	0.238	555	10.0	M10-02	9.27	0.219	0.224	525	9.99
M05-01	16.0	0.275	0.386	536	16.9	M10-03	9.96	0.148	0.236	531	10.4
M05-02	15.7	0.273	0.378	533	16.6	M10-04	10.5	0.139	0.249	534	11.0
M05-03	16.6	0.257	0.397	535	17.5	M10-05	10.1	0.148	0.243	538	10.6
M06-01	9.31	0.166	0.224	534	9.86	M10-06	8.68	0.109	0.206	536	9.04
M06-02	10.3	0.181	0.257	554	10.9	M10-07	9.95	0.172	0.243	541	10.5
M06-03	9.24	0.126	0.213	519	9.66	M10-08	8.97	0.177	0.218	536	9.56
M06-04	10.4	0.187	0.254	541	11.0	M11-01	8.74	0.156	0.214	543	9.26
M06-05	9.76	0.173	0.230	523	10.3	M11-02	9.41	0.174	0.224	526	9.98
M06-06	9.67	0.175	0.232	531	10.2	M11-03	10.1	0.168	0.247	544	10.7
M06-07	9.09	0.187	0.227	548	9.71	M11-04	11.1	0.198	0.270	537	11.8
M06-08	8.70	0.200	0.211	528	9.36	M11-05	10.1	0.172	0.237	522	10.7
M07-01	15.8	0.247	0.386	545	16.6	M12-01	11.2	0.185	0.268	534	11.8
M07-02	12.7	0.228	0.313	543	13.5	M12-02	10.2	0.186	0.246	535	10.8
M07-03	14.9	0.259	0.362	539	15.8	M12-03	9.47	0.166	0.229	536	10.0
M07-04	11.8	0.210	0.290	543	12.5	M12-04	9.09	0.175	0.223	541	9.67
M07-05	14.6	0.256	0.351	534	15.4	M12-05	9.33	0.214	0.229	535	10.0
M07-06	14.7	0.245	0.361	544	15.5	M12-06	9.84	0.196	0.242	541	10.5
M07-07	14.7	0.239	0.354	538	15.5	M12-07	8.87	0.165	0.213	531	9.42
M07-08	12.6	0.220	0.302	531	13.3	M12-08	9.71	0.185	0.236	537	10.3
M07-09	10.2	0.191	0.241	524	10.8	M12-09	14.4	0.227	0.341	530	15.2
M07-10	14.6	0.253	0.355	541	15.4	M12-10	14.9	0.249	0.362	538	15.7
M07-11	15.0	0.244	0.366	542	15.8	M12-11	11.1	0.197	0.268	536	11.8
M07-12	13.7	0.239	0.326	528	14.5	M12-12	12.7	0.215	0.304	533	13.4
M07-13	11.0	0.207	0.259	520	11.7	M12-13	15.4	0.241	0.373	539	16.2
M07-14	8.55	0.183	0.208	533	9.16	M12-14	14.4	0.247	0.346	534	15.2
M08-01	8.60	0.323	0.219	532	9.67	M12-15	12.5	0.222	0.301	535	13.2
M08-02	8.35	0.159	0.197	520	8.88	M12-16	10.6	0.181	0.250	525	11.2

Table 1. (Continued)

Grain No.	ThO ₂ (wt%)	UO ₂ (wt%)	PbO (wt%)	Age (Ma)	ThO ₂ * (wt%)	Grain No.	ThO ₂ (wt%)	UO ₂ (wt%)	PbO (wt%)	Age (Ma)	ThO ₂ * (wt%)
M12-17	10.1	0.174	0.242	533	10.7	M18-03	9.10	0.163	0.215	524	9.64
M12-18	10.7	0.196	0.260	538	11.3	M19-01	9.07	0.167	0.220	536	9.62
M12-19	10.9	0.198	0.263	537	11.6	M19-02	9.22	0.171	0.222	533	9.79
M20-20	9.35	0.155	0.226	539	9.86	M19-03	9.67	0.179	0.235	537	10.3
M13-01	12.8	0.204	0.299	522	13.5	M19-04	10.0	0.184	0.241	533	10.6
M13-02	13.4	0.220	0.323	536	14.1	M19-05	9.48	0.166	0.227	532	10.0
M13-03	11.8	0.195	0.282	534	12.4	M20-01	9.45	0.171	0.226	531	10.0
M13-04	11.0	0.169	0.260	529	11.6	M20-02	7.13	0.160	0.174	533	7.66
M13-05	9.84	0.168	0.237	535	10.4	M20-03	7.16	0.147	0.174	534	7.65
M14-01	10.8	0.183	0.261	536	11.4	M20-04	6.75	0.154	0.166	536	7.26
M14-02	11.6	0.187	0.282	541	12.2	M21-01	10.2	0.164	0.245	536	10.7
M14-03	11.2	0.186	0.268	533	11.8	M21-02	10.7	0.197	0.260	537	11.4
M14-04	10.2	0.175	0.243	529	10.8	M21-03	10.7	0.207	0.256	529	11.4
M14-05	9.56	0.159	0.228	530	10.1	M22-01	12.9	0.150	0.308	539	13.4
M15-01	10.3	0.185	0.249	534	10.9	M22-02	13.9	0.150	0.327	535	14.4
M15-02	10.2	0.166	0.246	536	10.8	M22-03	16.4	0.196	0.390	538	17.0
M15-03	10.3	0.164	0.245	534	10.8	M22-04	16.9	0.198	0.399	534	17.6
M15-04	10.9	0.173	0.260	535	11.5	M22-05	15.9	0.191	0.375	532	16.5
M16-01	8.93	0.160	0.218	540	9.46	M23-01	12.7	0.206	0.308	541	13.4
M16-02	9.52	0.163	0.223	521	10.1	M23-02	14.8	0.233	0.348	526	15.6
M16-03	9.44	0.172	0.227	534	10.0	M23-03	19.6	0.426	0.480	536	21.0
M16-04	9.28	0.166	0.220	527	9.83	M23-04	10.6	0.193	0.257	537	11.2
M16-05	8.32	0.171	0.206	545	8.89	M23-05	9.34	0.209	0.228	533	10.0
M17-01	8.97	0.162	0.215	531	9.51	M23-06	12.5	0.221	0.297	525	13.2
M17-02	10.6	0.189	0.256	535	11.2	M24-01	8.28	0.409	0.220	537	9.63
M17-03	9.74	0.166	0.232	530	10.3	M24-02	10.0	0.507	0.267	536	11.7
M17-04	9.73	0.169	0.239	544	10.3	M24-03	6.82	0.348	0.180	530	7.97
M17-05	9.86	0.162	0.239	539	10.4	M24-04	9.92	0.478	0.261	533	11.5
M18-01	8.21	0.148	0.198	533	8.70	M24-05	2.45	0.221	0.073	535	3.18
M18-02	9.03	0.162	0.220	541	9.57						

and SUZUKI (1992).

(1) Garnet-biotite gneiss (MA88011113-3)

A total of 151 spots on 24 matrix monazite grains from the Hesteskoen sample were analyzed. Monazites contain 2.01–19.6 wt% ThO₂, 0.109–0.507 wt% UO₂ and 0.061–0.480 wt% PbO (Table 1). On the PbO-ThO₂* diagram (Fig. 2), the data form a linear array and yield an isochron of 535.8 ± 3.7 Ma (MSWD=0.15) with an intercept value of -0.0003 ± 0.0016 .

(2) Gahnite-garnet-biotite gneiss (MA88012305-1)

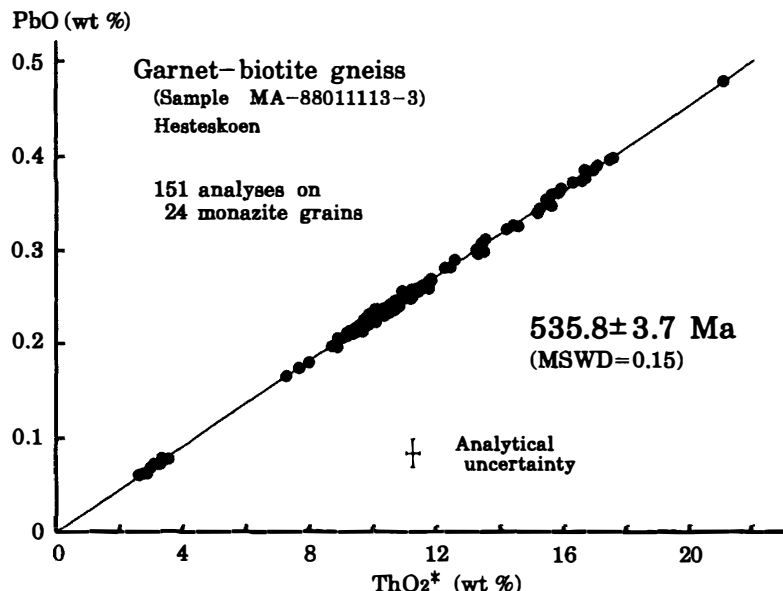
Monazite analyses of the southern Balchenfjella sample are from 13 grains in the matrix and 2 inclusions in garnet and pyrrhotite (Table 2). Monazites contain 1.08–6.43 wt% ThO₂, 0.044–0.582 wt% UO₂ and 0.040–0.179 wt% PbO (Table 2). A total of 118 analyses on 15 grains form a linear array and yield an isochron of

Table 2. Microprobe analyses of ThO_2 , UO_2 and PbO of monazites in gahnite-garnet-biotite gneiss (sample: MA88012305-1) from southern Balchenfjella. ThO_2^* : sum of the measured ThO_2 and ThO_2 equivalent of the measured UO_2 . Monazites M04 and M15 are inclusions in garnet (Gt) and pyrrhotite (Oq), respectively.

Grain No.	ThO_2 (wt%)	UO_2 (wt%)	PbO (wt%)	Age (Ma)	ThO_2^* (wt%)	Gain No.	ThO_2 (wt%)	UO_2 (wt%)	PbO (wt%)	Age (Ma)	ThO_2^* (wt%)
M01-01	3.24	0.205	0.090	538	3.92	M04-10	4.32	0.270	0.118	532	5.21
M01-02	3.09	0.133	0.079	524	3.53	M04-11	3.43	0.289	0.099	528	4.39
M01-03	2.93	0.103	0.073	523	3.27	M04-12	2.96	0.198	0.084	544	3.62
M01-04	2.92	0.179	0.080	537	3.51	M04-13	3.25	0.306	0.097	535	4.26
M01-05	2.18	0.127	0.060	536	2.60	M04-14	6.43	0.424	0.179	537	7.83
M01-06	3.12	0.121	0.077	514	3.52	M04-15	3.10	0.182	0.085	539	3.70
M02-01	3.36	0.086	0.082	527	3.65	M04-16	2.89	0.122	0.074	530	3.29
M02-02	3.29	0.078	0.081	538	3.55	M05-01	2.31	0.156	0.065	537	2.83
M02-03	3.88	0.051	0.092	531	4.05	M05-02	2.96	0.113	0.074	523	3.33
M02-04	2.40	0.391	0.084	531	3.69	M05-03	2.19	0.313	0.075	544	3.23
M02-05	3.26	0.076	0.081	539	3.51	M05-04	2.96	0.140	0.078	534	3.42
M02-06	2.72	0.447	0.096	535	4.20	M05-05	3.29	0.129	0.084	533	3.72
M02-07	2.96	0.582	0.111	535	4.89	M05-06	3.36	0.128	0.087	542	3.78
M02-08	2.21	0.469	0.085	528	3.76	M05-07	1.85	0.281	0.059	501	2.78
M02-09	2.21	0.458	0.081	509	3.72	M05-08	2.26	0.264	0.072	538	3.14
M02-10	1.97	0.500	0.082	533	3.63	M05-09	2.94	0.149	0.078	533	3.43
M02-11	3.22	0.100	0.079	524	3.55	M05-10	2.06	0.382	0.077	544	3.33
M02-12	3.31	0.089	0.080	522	3.60	M05-11	2.44	0.366	0.082	524	3.65
M02-13	3.16	0.100	0.080	541	3.49	M05-12	1.49	0.253	0.056	567	2.33
M02-14	3.34	0.069	0.081	535	3.57	M05-13	2.49	0.180	0.068	516	3.09
M02-15	3.40	0.074	0.082	531	3.65	M05-14	2.60	0.174	0.069	511	3.17
M03-01	1.28	0.401	0.060	537	2.61	M06-01	1.80	0.334	0.066	532	2.91
M03-02	2.07	0.399	0.077	531	3.39	M06-02	1.75	0.126	0.050	539	2.17
M03-03	1.49	0.464	0.069	532	3.03	M06-03	2.41	0.114	0.061	514	2.79
M03-04	1.20	0.400	0.057	534	2.52	M06-04	3.72	0.049	0.088	533	3.88
M03-05	1.53	0.258	0.053	520	2.39	M06-05	1.76	0.339	0.063	516	2.88
M03-06	1.46	0.428	0.067	545	2.88	M06-06	1.66	0.212	0.054	532	2.36
M03-07	1.43	0.468	0.068	538	2.98	M06-07	2.64	0.109	0.067	527	3.00
M03-08	1.59	0.459	0.072	543	3.11	M07-01	3.50	0.057	0.084	534	3.69
M03-09	1.95	0.388	0.073	527	3.23	M07-02	5.47	0.391	0.156	541	6.77
M03-10	1.45	0.499	0.069	523	3.10	M07-03	5.67	0.361	0.156	534	6.87
M03-11	1.68	0.314	0.062	530	2.72	M07-04	5.04	0.538	0.155	535	6.82
M03-12	1.08	0.364	0.053	544	2.29	M07-05	5.02	0.334	0.140	535	6.13
M03-13	1.13	0.365	0.053	532	2.34	M07-06	4.74	0.325	0.132	531	5.82
M03-14	1.13	0.389	0.056	541	2.42	M07-07	3.91	0.272	0.108	527	4.81
M03-15	1.88	0.234	0.062	547	2.66	M08-01	1.47	0.375	0.061	526	2.71
M04-01 Gt	3.45	0.256	0.096	527	4.30	M08-02	2.42	0.157	0.070	556	2.94
M04-02	3.47	0.153	0.092	541	3.98	M08-03	2.56	0.179	0.070	523	3.15
M04-03	3.58	0.331	0.108	543	4.68	M08-04	1.47	0.369	0.061	530	2.69
M04-04	4.23	0.320	0.118	526	5.29	M08-05	2.44	0.213	0.070	521	3.14
M04-05	4.01	0.341	0.118	538	5.14	M09-01	1.37	0.213	0.048	539	2.08
M04-06	3.02	0.259	0.086	520	3.88	M09-02	1.62	0.283	0.058	535	2.56
M04-07	3.03	0.187	0.086	553	3.65	M09-03	1.96	0.364	0.073	538	3.17
M04-08	5.36	0.333	0.148	539	6.46	M09-04	2.40	0.181	0.067	525	3.00
M04-09	5.83	0.331	0.157	531	6.93	M09-05	1.62	0.281	0.058	536	2.55

Table 2. (Continued)

Grain No.	ThO ₂ (wt%)	UO ₂ (wt%)	PbO (wt%)	Age (Ma)	ThO ₂ * (wt%)	Grain No.	ThO ₂ (wt%)	UO ₂ (wt%)	PbO (wt%)	Age (Ma)	ThO ₂ * (wt%)
M10-01	2.34	0.284	0.075	537	3.28	M14-01	3.00	0.085	0.077	549	3.28
M10-02	2.38	0.181	0.068	539	2.98	M14-02	2.97	0.104	0.076	540	3.31
M10-03	2.09	0.289	0.070	540	3.05	M14-03	1.38	0.244	0.049	521	2.19
M10-04	2.28	0.123	0.066	575	2.69	M14-04	2.48	0.110	0.065	534	2.84
M10-05	1.99	0.264	0.063	516	2.86	M14-05	3.03	0.103	0.080	558	3.37
M11-01	1.17	0.187	0.040	527	1.79	M14-06	1.08	0.306	0.049	544	2.09
M11-02	2.50	0.044	0.060	529	2.65	M15-01 Oq	2.66	0.084	0.068	542	2.94
M12	2.01	0.099	0.055	549	2.34	M15-02	2.54	0.152	0.069	532	3.04
M13-01	2.80	0.109	0.073	543	3.16	M15-03	2.61	0.162	0.072	534	3.15
M13-02	2.57	0.097	0.066	534	2.89	M15-04	2.23	0.150	0.063	543	2.73
M13-03	3.24	0.044	0.078	538	3.38	M15-05	2.23	0.108	0.058	528	2.59
M13-04	3.01	0.118	0.076	527	3.40	M15-06	2.22	0.145	0.060	523	2.70
M13-05	2.92	0.086	0.074	541	3.21	M15-07	2.26	0.186	0.069	565	2.88
M13-06	2.83	0.112	0.073	538	3.20	M15-08	2.65	0.059	0.066	546	2.85

Fig. 2. PbO-ThO₂* plot of monazite grains in garnet-biotite gneiss (MA88011113-3) from Hestekoen.

534.2±5.8 Ma (MSWD=0.07) with an intercept value of 0.0001±0.0009 (Fig. 3).
(3) Sillimanite-garnet-biotite gneiss (MA88012912)

Analyzed monazites in the Austhjelmen sample are matrix grains, and contain 1.37–8.69 wt% ThO₂, 0.241–0.741 wt% UO₂ and 0.047–0.224 wt% PbO (Table 3). A total of 88 data points on 14 monazite grains yield an isochron of 534.0±6.3 Ma (MSWD=0.07) with an intercept value of -0.0010±0.0016 (Fig. 4).

Table 3. Microprobe analyses of ThO_2 , UO_2 and PbO of monazites in sillimanite-garnet-biotite gneiss (sample: MA88012912) from Austhjelmen. ThO_2^* : sum of the measured ThO_2 and ThO_2 equivalent of the measured UO_2 .

Grain No.	ThO_2 (wt%)	UO_2 (wt%)	PbO (wt%)	Age (Ma)	ThO_2^* (wt%)	Grain No.	ThO_2 (wt%)	UO_2 (wt%)	PbO (wt%)	Age (Ma)	ThO_2^* (wt%)
M01-01	5.88	0.351	0.157	525	7.04	M06-12	4.05	0.359	0.119	535	5.24
M01-02	6.13	0.266	0.157	527	7.01	M06-13	3.79	0.389	0.113	522	5.08
M01-03	6.25	0.260	0.161	533	7.11	M06-14	4.31	0.379	0.125	527	5.56
M01-04	6.30	0.268	0.161	527	7.19	M06-15	4.19	0.373	0.122	530	5.42
M01-05	6.66	0.279	0.171	530	7.58	M06-16	4.34	0.392	0.126	524	5.64
M01-06	8.69	0.373	0.224	530	9.93	M07-01	2.65	0.624	0.105	521	4.72
M01-07	8.39	0.384	0.222	539	9.66	M07-02	3.17	0.550	0.116	544	4.99
M01-08	6.54	0.379	0.176	531	7.80	M07-03	1.37	0.241	0.047	515	2.17
M02-01	4.96	0.512	0.153	540	6.66	M08-01	4.09	0.421	0.123	525	5.48
M02-02	5.29	0.344	0.145	531	6.43	M08-02	3.89	0.364	0.114	528	5.10
M02-03	5.36	0.373	0.144	514	6.60	M08-03	3.23	0.289	0.095	535	4.19
M02-04	4.42	0.355	0.125	526	5.60	M08-04	3.56	0.311	0.103	529	4.59
M02-05	4.23	0.318	0.118	524	5.28	M08-05	3.79	0.378	0.115	536	5.04
M02-06	4.22	0.324	0.118	523	5.29	M08-06	3.86	0.383	0.117	536	5.13
M02-07	4.90	0.338	0.136	531	6.02	M08-07	3.86	0.389	0.116	530	5.15
M02-08	4.93	0.321	0.134	526	5.99	M08-08	3.86	0.386	0.117	532	5.14
M02-09	4.47	0.276	0.124	539	5.38	M08-09	3.76	0.386	0.111	518	5.04
M02-10	4.27	0.285	0.116	524	5.21	M08-10	3.45	0.336	0.103	530	4.56
M02-11	4.72	0.315	0.130	531	5.76	M08-11	3.95	0.411	0.120	528	5.31
M02-12	3.94	0.306	0.112	532	4.95	M08-12	3.77	0.375	0.113	532	5.01
M03-01	3.85	0.444	0.119	524	5.32	M08-13	3.38	0.323	0.100	528	4.45
M03-02	4.18	0.461	0.128	528	5.71	M08-14	3.80	0.336	0.109	523	4.91
M03-03	3.94	0.393	0.121	542	5.24	M09-01	4.98	0.444	0.145	527	6.45
M03-04	4.08	0.425	0.126	540	5.49	M09-02	5.93	0.452	0.168	532	7.43
M04-01	6.43	0.327	0.170	532	7.51	M09-03	5.65	0.458	0.159	522	7.17
M04-02	6.49	0.346	0.174	535	7.64	M09-04	4.72	0.458	0.138	521	6.24
M04-03	6.51	0.336	0.170	524	7.62	M10-01	5.60	0.402	0.157	531	6.93
M04-04	6.71	0.336	0.178	535	7.82	M10-02	5.83	0.422	0.163	531	7.23
M04-05	6.68	0.338	0.174	524	7.80	M10-03	5.61	0.426	0.159	530	7.02
M04-06	6.33	0.416	0.176	537	7.71	M11-01	4.52	0.388	0.131	528	5.80
M04-07	6.37	0.339	0.169	530	7.49	M11-02	4.52	0.408	0.132	527	5.87
M05-01	5.28	0.583	0.164	535	7.21	M11-03	5.01	0.398	0.145	537	6.33
M05-02	6.03	0.513	0.175	532	7.73	M11-04	5.16	0.393	0.144	523	6.46
M06-01	4.64	0.378	0.133	530	5.89	M12-01	2.43	0.472	0.091	535	3.99
M06-02	4.33	0.375	0.123	520	5.57	M12-02	1.78	0.379	0.069	533	3.04
M06-03	3.96	0.378	0.119	536	5.21	M13-01	4.80	0.374	0.138	534	6.04
M06-04	3.96	0.356	0.118	540	5.14	M13-02	3.24	0.278	0.093	525	4.16
M06-05	4.46	0.423	0.131	525	5.86	M13-03	5.50	0.346	0.151	533	6.65
M06-06	3.63	0.373	0.111	536	4.86	M13-04	5.04	0.412	0.144	528	6.41
M06-07	4.62	0.444	0.139	534	6.09	M13-05	4.49	0.396	0.130	524	5.80
M06-08	4.42	0.426	0.131	529	5.83	M14-01	5.09	0.540	0.155	529	6.88
M06-09	4.33	0.372	0.125	528	5.56	M14-02	4.73	0.741	0.164	537	7.18
M06-10	4.76	0.337	0.135	539	5.88	M14-03	6.45	0.271	0.165	529	7.35
M06-11	4.36	0.316	0.121	524	5.41	M14-04	6.21	0.269	0.159	527	7.10

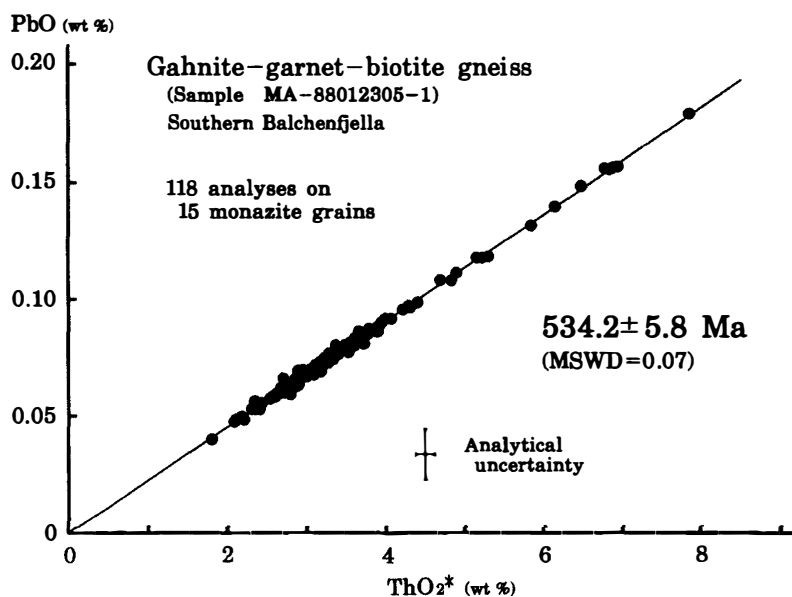


Fig. 3. PbO - ThO_2^* plot of monazite grains in gahnite-garnet-biotite gneiss (MA88012305-1) from southern Balchenfjella.

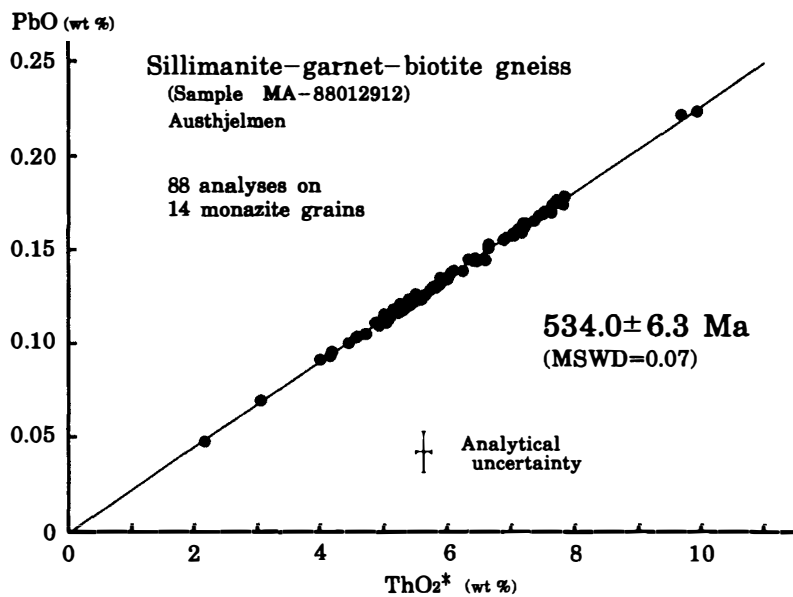


Fig. 4. PbO - ThO_2^* plot of monazite grains in sillimanite-garnet-biotite gneiss (MA88012912) from Austhjelmen.

6. Discussion

The PbO - ThO_2^* plots for each sample (Figs. 2 to 4) give well-defined isochrons with no indication of older or younger ages, although monazites both in the matrix and enclosed in garnet and pyrrhotite grains were analyzed. Moreover, the resultant

CHIME ages, 536, 534 and 534 Ma, are not significantly different. These features indicate a single crystallization age (*ca.* 535 Ma) of the monazites.

Many isotopic ages have been measured on the Sør Rondane metamorphic and plutonic rocks using various methods. The early work by PICCIOTTO *et al.* (1964), VAN AUTENBOER (1969) and PASTEELS and MICHOT (1970) reveals that most of the Rb-Sr mineral and whole-rock ages and U-Pb zircon and sphene ages are restricted to the early Paleozoic time (460–550 Ma). Recent geochronologic studies, however, gave older ages around 1000 Ma in addition to *ca.* 500 Ma ages (Table 4). As stated above, the majority of metamorphic rocks in the mountains has undergone granulite-facies regional metamorphism, followed by amphibolite-facies recrystallization. On the basis of the geologic and petrologic backgrounds, the ages around 1000 Ma have been interpreted as the time of the regional granulite-facies event, and those around 500 Ma as the time of the retrograde contact metamorphism related to granitic activity and amphibolite-facies recrystallization associated with migmatization (ASAMI *et al.*, 1992; GREW *et al.*, 1992; SHIRAISHI and KAGAMI, 1992).

The 534–536 Ma CHIME monazite ages obtained in this study are in good agreement with the above ~500 Ma isotopic ages. Since the studied samples show evidence of the retrograde amphibolite-facies overprint, the monazite grains could be interpreted either to have formed during the retrograde event, or to have lost all their radiogenic Pb during the retrograde event. However, the retrograde formation of monazite is unlikely; petrographic characteristics such as the presence of monazite

Table 4. Recent geochronologic data on the Sør Rondane metamorphic and plutonic rocks. K-Ar ages are excluded.

Age (Ma)	Method	Rock sample	Source
<i>Older</i>			
1110	UI U-Pb Zrn	Gneisses	GREW <i>et al.</i> (1992)
978	Rb-Sr WR _I	Granulites	SHIRAISHI and KAGAMI (1992)
961	Sm-Nd WR _I	Granulites	<i>Ditto</i>
956	Rb-Sr WR _I	Tonalites	TAKAHASHI <i>et al.</i> (1990)
<i>Younger</i>			
439	Ar-Ar WR	Metadolerite	TAKIGAMI <i>et al.</i> (1987)
458	LI U-Pb Zrn	Gneisses	GREW <i>et al.</i> (1992)
455, 457, 458, 479	Rb-Sr M _I	Gneisses	<i>Ditto</i>
489	Rb-Sr M _I	Granulite	SHIRAISHI and KAGAMI (1992)
624	Sm-Nd M _I	Granulite	<i>Ditto</i>
525	Rb-Sr WR _I	Granites	TAKAHASHI <i>et al.</i> (1990)
496, 499, 500, 501	Ar-Ar Bt	Granites	TAKIGAMI and FUNAKI (1991)
487	Ar-Ar Bt	Granite	TAKIGAMI <i>et al.</i> (1992)
506, 528	Rb-Sr WR _I	Granites	TAINOSHIO <i>et al.</i> (1992)
519	Sm-Nd WR _I	Granites	ARAKAWA <i>et al.</i> (1994)

UI: upper intercept, LI: lower intercept. Bt: biotite, Zrn: zircon. M_I: mineral isochron, WR: whole rock, WR_I: whole-rock isochron.

grains in Mg-rich cores of garnet implies monazite formed during the granulite-facies event.

The second possibility, entire resetting of the granulite-stage monazite during the amphibolite-facies overprint, is also unlikely judging from the following observations. SMITH and BARREIRO (1990) reported that monazite in metapelites formed as a metamorphic mineral in the staurolite-zone of prograde metamorphism (525°C , 3.1 kb), initiating its role as a chronometer, and remained a closed system even when subsequent metamorphism attained upper-sillimanite-zone conditions. Survival of detrital monazite grains with middle Precambrian ages in late Permian and Cretaceous upper amphibolite-facies regional metamorphic rocks (SUZUKI and ADACHI, 1994; SUZUKI *et al.*, 1994) is another piece of supporting evidence for high Pb retentivity of monazite. The closure temperature of monazite for Pb, as high as 725°C , requires prolonged heating under uppermost amphibolite-facies or granulite-facies conditions in order to lose Pb (PARRISH, 1990). These observations suggest that the total loss of Pb from monazite would not occur during the amphibolite-facies ($\sim 550^{\circ}\text{C}$) overprint in the map area. Consequently, we consider that the 534–536 Ma CHIME monazite ages represent the time of the monazite formation either during the prograde stage or at the thermal peak ($\sim 780^{\circ}\text{C}$) of the granulite-facies regional metamorphism.

As mentioned above, the older ages, 1110 Ma from the mapped area and both 978 and 961 Ma from Bratnipane 80 km west of the area, have been cited as evidence for a late Proterozoic regional granulite-facies event. These ages are similar or very close to the Nd depleted mantle model ages on the gneisses and granulites from which the older ages were obtained, and such results constrain crustal prehistory prior to the granulite-facies event to an extremely short interval (GREW *et al.*, 1992; SHIRAISHI and KAGAMI, 1992). Alternatively, it is possible to regard the older ages as representing the emplacement of protoliths of these high-grade rocks, as pointed out by SHIRAISHI and KAGAMI (1992), or the 1110 Ma as representing an age of detrital zircons, an explanation suggested for zircon ages (~ 950 Ma) from the central and western Sør Rondane gneisses (PASTEELS and MICHOT, 1970).

New studies have indicated the existence of a Cambrian orogenic belt within the East Antarctic Shield on the basis of ion microprobe zircon-rim ages of 520–600 Ma (SHIRAISHI *et al.*, 1992, 1994). The belt includes at least the Lützow-Holm and Yamato-Belgica Complexes, which are located about 200–500 km east of the Sør Rondane Mountains. Rocks in this belt record an upper amphibolite- to granulite-facies regional metamorphic event followed by plutonic activity and associated retrograde metamorphism, similar to the situation in the Sør Rondane. Our ~ 535 Ma monazite ages from the eastern Sør Rondane give rise to a possibility of further westward extension of the Cambrian belt, and of increased significance of Pan-African tectono-thermal activity in the East Antarctic margin and the Gondwana crustal evolution.

Acknowledgments

We are indebted to E.S. GREW of the University of Maine and T. TANAKA of

Nagoya University for reviewing an earlier draft of this paper. We are grateful to S. YOGO of Nagoya University for preparing polished thin sections for microprobe analyses. M. ASAMI would like to thank H. MAKIMOTO of the Geological Survey of Japan and E.S. GREW for their collaborative field work during JARE-29. This research was supported by a Grant-in-Aid for Scientific Research (C) of the Ministry of Education, Science, Sports and Culture, Japan (No. 08640609).

References

- ADACHI, M. and SUZUKI, K. (1992): A preliminary note on the age of detrital monazites and zircons from sandstones in the Upper Triassic Nabae Group, Maizuru terrane. *Mem. Geol. Soc. Jpn.*, **38**, 111–120.
- ARAKAWA, Y., TAKAHASHI, Y. and TAINOSHIO, Y. (1994): Nd and Sr isotope characteristics of the plutonic rocks in the Sør Rondane Mountains, East Antarctica. *Proc. NIPR Symp. Antarct. Geosci.*, **7**, 49–59.
- ASAMI, M. and MAKIMOTO, H. (1991): Granulite-facies metamorphic conditions in the eastern Sør Rondane Mountains, East Antarctica (abstract). *Proc. NIPR Symp. Antarct. Geosci.*, **5**, 166.
- ASAMI, M., MAKIMOTO, H. and GREW, E. S. (1989): Geology of the eastern Sør Rondane Mountains, East Antarctica. *Proc. NIPR Symp. Antarct. Geosci.*, **3**, 81–99.
- ASAMI, M., GREW, E. S. and MAKIMOTO, H. (1990): A staurolite-bearing corundum-garnet gneiss from the eastern Sør Rondane Mountains, Antarctica. *Proc. NIPR Symp. Antarct. Geosci.*, **4**, 22–40.
- ASAMI, M., MAKIMOTO, H., GREW, E. S., OSANAI, Y., TAKAHASHI, Y., TSUCHIYA, N., TAINOSHIO, Y. and SHIRAISHI, K. (1991): Geological map of Balchenfjella, Sør Rondane Mountains, Antarctica. *Antarct. Geol. Map Ser.*, Sheet 31 (with explanatory text 11p., 8pl.), Tokyo, Natl Inst. Polar Res.
- ASAMI, M., OSANAI, Y., SHIRAISHI, K. and MAKIMOTO, H. (1992): Metamorphic Evolution of the Sør Rondane Mountains, East Antarctica. *Recent Progress in Antarctic Earth Science*, ed. by Y. YOSHIDA *et al.* Tokyo, Terra Sci. Publ., 7–15.
- ASAMI, M., GREW, E. S. and MAKIMOTO, H. (1993): Contrasting mineral associations between two wollastonite-bearing calc-silicate gneisses, eastern Sør Rondane Mountains, Antarctica. *Proc. NIPR Symp. Antarct. Geosci.*, **6**, 57–71.
- ASAMI, M., MAKIMOTO, H. and GREW, E. S. (1994): Relict sapphirine in pyropic garnet from the eastern Sør Rondane Mountains, Antarctica (abstract). *Proc. NIPR Symp. Antarct. Geosci.*, **7**, 179.
- BENCE, A. E. and ALBEE, A. L. (1968): Empirical correction factors for the electron microanalysis of silicates and oxides. *J. Geol.*, **76**, 382–403.
- GREW, E. S., ASAMI, M. and MAKIMOTO, H. (1988): Field studies in the eastern Sør Rondane Mountains, East Antarctica, with the 29th Japanese Antarctic Research Expedition (JARE). *Antarct. J. U. S.*, **23**(5), 44–46.
- GREW, E. S., ASAMI, M. and MAKIMOTO, H. (1989a): Preliminary petrological studies of the metamorphic rocks of the eastern Sør Rondane Mountains. *Proc. NIPR Symp. Antarct. Geosci.*, **3**, 100–127.
- GREW, E. S., ASAMI, M. and MAKIMOTO, H. (1989b): Aluminous and manganoan titanite from the Sør Rondane Mountains, East Antarctica. *Antarct. J. U. S.*, **24**(5), 42–43.
- GREW, E. S., ESSENE, E. J., PEACOR, D. R., SU, S. and ASAMI, M. (1991): Dissakisite-(Ce), a new member of the epidote group and the Mg analogue of allanite-(Ce), from Antarctica. *Am. Mineral.*, **76**, 1990–1997.
- GREW, E. S., MANTON, W. I., ASAMI, M. and MAKIMOTO, H. (1992): Geochronologic data on Proterozoic polymetamorphic rocks of the eastern Sør Rondane Mountains, East Antarctica. *Recent Progress in Antarctic Earth Science*, ed. by Y. Yoshida *et al.* Tokyo, Terra Sci. Publ., 37–44.
- ISHIZUKA, H., ASAMI, M., GREW, E. S., KOJIMA, H., MAKIMOTO, H., MORIWAKI, Y., OSANAI, Y., OWADA, M., SAKIYAMA, T., SHIRAISHI, K., TAINOSHIO, Y., TAKAHASHI, Y., TOYOSHIMA, T. and TSUCHIYA, N. (1993): Geological map of Bergersenfjella, Sør Rondane Mountains, Antarctica. *Antarct. Geol. Map Ser.*, Sheet 33 (with explanatory text 10p., 5pl.), Tokyo, Natl Inst. Polar Res.

- MAKIMOTO, H., ASAMI, M. and GREW, E. S. (1990): Metamorphic conditions of ultramafic lenses from the eastern Sør Rondane Mountains, East Antarctica. *Proc. NIPR Symp. Antarct. Geosci.*, **4**, 9–21.
- PARRISH, R. R. (1990): U-Pb dating of monazite and its application to geological problems. *Can. J. Earth Sci.*, **27**, 1431–1450.
- PASTEELS, P. and MICHOT, J. (1970): Uranium-lead radioactive dating and lead isotope study on sphene and K-feldspar in the Sør-Rondane Mountains, Dronning Maud Land, Antarctica. *Eclogae Geol. Helv.*, **63**, 239–254.
- PICCIOTTO, E., DEUTSCH, S. and PASTEELS, P. (1964): Isotopic ages from the Sør-Rondane Mountains, Dronning Maud Land. *Antarctic Geology*, ed. R.J. ADIE. Amsterdam, North-Holland Publ., 570–578.
- SHIRAIKI, K. and KAGAMI, H. (1992): Sm-Nd and Rb-Sr ages of metamorphic rocks from the Sør Rondane Mountains, East Antarctica. *Recent Progress in Antarctic Earth Science*, ed. by Y. YOSHIDA *et al.* Tokyo, Terra Sci. Publ., 29–35.
- SHIRAIKI, K., ASAMI, M., ISHIZUKA, H., KOJIMA, H., KOJIMA, S., OSANAI, Y., SAKIYAMA, T., TAKAHASHI, Y., YAMAZAKI, M. and YOSHIKURA, S. (1991): Geology and metamorphism of the Sør Rondane Mountains, East Antarctica. *Geological Evolution of Antarctica*, ed. by M.R.A. THOMSON *et al.* Cambridge, Cambridge Univ. Press, 77–82.
- SHIRAIKI, K., HIROI, Y., ELLIS, D. J., FANNING, C. M., MOTYOYOH, Y. and NAKAI, Y. (1992): The first report of a Cambrian orogenic belt in East Antarctica—An ion microprobe study of the Lützow-Holm Complex. *Recent Progress in Antarctic Earth Science*, ed. by Y. YOSHIDA *et al.* Tokyo, Terra Sci. Publ., 67–73.
- SHIRAIKI, K., ELLIS, D. J., HIROI, Y., FANNING, C. M., MOTYOYOH, Y. and NAKAI, Y. (1994): Cambrian orogenic belt in East Antarctica and Sri Lanka: Implication for Gondwana assembly. *J. Geol.*, **102**, 47–65.
- SMELLIE, J. A. T., COGGER, N. and HERRINGTON, J. (1978): Standards for quantitative microprobe determination of uranium and thrium with additional information on the chemical formulae of dawsonite and euxenite-polycrase. *Chem. Geol.*, **22**, 1–10.
- SMITH, H. A. and BARREIRO, B. (1990): Monazite U-Pb dating of staurolite grade metamorphism in pelitic schist. *Contrib. Mineral. Petrol.*, **105**, 602–615.
- SUZUKI, K. and ADACHI, M. (1991a): Precambrian provenance and Silurian metamorphism of the Tsubonosawa paragneiss in the South Kitakami terrane, Northeast Japan, revealed by the chemical Th-U-total Pb isochron ages of monazite, zircon and xenotime. *Geochem. J.*, **25**, 357–376.
- SUZUKI, K. and ADACHI, M. (1991b): The chemical Th-U-total Pb isochron ages of zircon and monazite from the Gray Granite of the Hida terrane, Japan. *J. Earth Sci., Nagoya Univ.*, **38**, 11–37.
- SUZUKI, K. and ADACHI, M. (1994): Middle Precambrian detrital monazite and zircon from the Hida gneiss on Oki-Dogo Island, Japan: Their origin and implications for the correlation of basement gneiss of Southwest Japan and Korea. *Tectonophysics*, **235**, 277–292.
- SUZUKI, K., ADACHI, M. and TANAKA, T. (1991): Middle Precambrian provenance of Jurassic sandstone in the Mino terrane, central Japan: Th-U-total Pb evidence from an electron microprobe monazite study. *Sediment. Geol.*, **75**, 141–147.
- SUZUKI, K., ADACHI, M., SANGO, K. and CHIBA, H. (1992): Chemical Th-U-total Pb isochron ages of monazites and zircons from the Hikami Granite and “Siluro-Devonian” clastic rocks in the South Kitakami terrane. *J. Mineral. Petrol. Econ. Geol.*, **87**, 330–349 (in Japanese with English abstract).
- SUZUKI, K., ADACHI, M. and KAJIZUKA, I. (1994): Electron microprobe observations of Pb diffusion in metamorphosed detrital monazites. *Earth Planet. Sci. Lett.*, **128**, 391–405.
- TAINOSH, Y., TAKAHASHI, Y., ARAKAWA, Y., OSANAI, Y., TSUCHIYA, N., SAKIYAMA, T. and OWADA, M. (1992): Petrochemical character and Rb-Sr isotopic investigation of the granitic rocks from the Sør Rondane Mountains, East Antarctica. *Recent Progress in Antarctic Earth Science*, ed. by Y. YOSHIDA *et al.* Tokyo, Terra Sci. Publ., 45–54.
- TAKAHASHI, Y., ARAKAWA, Y., SAKIYAMA, T., OSANAI, Y. and MAKIMOTO, H. (1990): Rb-Sr and K-Ar whole rock ages of the plutonic bodies from the Sør Rondane Mountains, East Antarctica. *Proc.*

- NIPR Symp. Antarct. Geosci., **4**, 1–8.
- TAKIGAMI, Y. and FUNAKI, M. (1991): ^{40}Ar - ^{39}Ar ages for igneous and metamorphic rocks from the Sør Rondane Mountains, East Antarctica. Proc. NIPR Symp. Antarct. Geosci., **5**, 122–135.
- TAKIGAMI, Y., KANEOKA, I. and FUNAKI, M. (1987): Age and paleomagnetic studies for intrusive and metamorphic rocks from the Sør Rondane Mountains, Antarctica. Proc. NIPR Symp. Antarct. Geosci., **1**, 169–177.
- TAKIGAMI, Y., FUNAKI, M. and TOKIEDA, K. (1992): ^{40}Ar - ^{39}Ar geochronological studies on some paleomagnetic samples of East Antarctica. Recent Progress in Antarctic Earth Science, ed. by Y. YOSHIDA *et al.* Tokyo, Terra Sci. Publ., 61–66.
- Van Autenboer, T. (1969): Geology of the Sør Rondane Mountins, Sheet 8, Sør Rondane Mountains. Geologic Maps of Antarctica, ed. by V. C. BUSHNELL and C. CRADDOCK. New York, Am. Geogr. Soc. (Antarct. Map Folio Ser., 12).
- VAN AUTENBOER, T. and LOY, W. (1972): Recent geological investigations in the Sør-Rondane Mountains, Belgicafjella and Sverdrupfjella, Dronning Maud Land. Antarctic Geology and Geophysics, ed. by R. J. ADIE. Oslo, Universitetsforlaget, 563–571.

(Received April 15, 1996; Revised manuscript accepted July 12, 1996)